Effects of oxygen-inserted layers on diffusion of boron, phosphorus, and arsenic in silicon for ultra-shallow junction formation

X. Zhang,[1,a)] D. Connelly,[1,2] H. Takeuchi,[2] M. Hytha,[2] R. J. Mears,[2] L. M. Rubin,[3] and T.-J. K. Liu[1]
[1]*Department of Electrical Engineering and Computer Sciences, University of California, Berkeley, California 94720, USA*
[2]*Atomera, Inc., Los Gatos, California 95035, USA*
[3]*Axcelis Technologies, Inc., Beverly, Massachusetts 01915, USA*

(Received 10 January 2018; accepted 15 March 2018; published online 29 March 2018)

The effects of oxygen-inserted (OI) layers on the diffusion of boron (B), phosphorus (P), and arsenic (As) in silicon (Si) are investigated, for ultra-shallow junction formation by high-dose ion implantation followed by rapid thermal annealing. The projected range (R_p) of the implanted dopants is shallower than the depth of the OI layers. Secondary ion mass spectrometry is used to compare the dopant profiles in silicon samples that have OI layers against the dopant profiles in control samples that do not have OI layers. Diffusion is found to be substantially retarded by the OI layers for B and P, and less for As, providing shallower junction depth. The experimental results suggest that the OI layers serve to block the diffusion of Si self-interstitials and thereby effectively reduce interstitial-aided diffusion beyond the depth of the OI layers. The OI layers also help to retain more dopants within the Si, which technology computer-aided design simulations indicate to be beneficial for achieving shallower junctions with lower sheet resistance to enable further miniaturization of planar metal-oxide-semiconductor field-effect transistors for improved integrated-circuit performance and cost per function. *Published by AIP Publishing*. https://doi.org/10.1063/1.5022078

I. INTRODUCTION

Planar bulk-silicon complementary metal-oxide-semiconductor (CMOS) field-effect transistor (FET) technology is predominantly used to produce semiconductor integrated circuits today.[1] MOSFET scaling to shorter gate length (below 30 nm) is desirable for improved transistor performance characteristics (i.e., higher on-state current and lower capacitance for faster and more energy-efficient circuit operation), but requires commensurate scaling of the source/drain junction depths. Specifically, the depth of the source/drain extension regions must be smaller than the gate length to mitigate short-channel effects while maintaining a high active dopant concentration to mitigate parasitic series resistance.[2–4] Typically, the dopants are introduced by ion implantation to form source/drain extension regions self-aligned to the edges of the gate electrode. During the subsequent thermal annealing process used to activate the implanted dopants, transient enhanced diffusion (TED) can occur due to point defects created during the implantation process,[5] resulting in a "tail" in the concentration *vs.* depth profile of boron[6–8] and a distinctive "kink-and-tail" profile of phosphorus,[9,10] which makes it difficult to achieve ultra-shallow junctions. Traditionally, arsenic is used to form ultra-shallow n-type regions in p-type silicon because it has lower diffusivity than does phosphorus[6] and also is less susceptible to TED.[11]

Partial monolayers of oxygen incorporated within a silicon substrate[12,13] recently have been demonstrated to be effective for retarding boron diffusion to achieve a super-steep retrograde channel doping profile, which is beneficial for suppressing short-channel effects and for reducing random-dopant fluctuation effects, in n-channel MOSFETs.[12] In this work, the efficacy of such "oxygen-inserted" (OI) layers for retarding the diffusion of dopants introduced by high-dose ion implantation (above the amorphization limit[14]) to achieve ultra-shallow doping profiles suitable for the formation of p+/n and n+/p junctions is investigated, for the first time.

II. EXPERIMENTAL

Experiments were performed using control and OI p-type silicon (Si) wafer substrates with (001) crystalline surface orientation. The OI substrates comprise multiple partial monolayers of oxygen starting at a depth of approximately 10 nm beneath the surface. The inserted oxygen atoms reside in interstitial sites, with each one covalently bonded to two neighboring Si atoms – a configuration that can withstand high-temperature processing (as shown below) and impede diffusion of silicon self-interstitials.[13]

The boron (B) doped samples were prepared by first counter-doping the wafer substrates (to convert them to be n-type near the surface) with a 90 keV, 2×10^{13} cm^{-2} arsenic ion implant.[15] Subsequently, BF_2 ions were implanted with an acceleration energy of 2.5 keV, at a dose of 1×10^{15} cm^{-2}. The phosphorus (P) doped samples were prepared by implanting P ions with an acceleration energy of 1 keV, at a dose of 1×10^{15} cm^{-2}. The arsenic (As) doped samples were prepared by implanting As ions with an acceleration energy of 1 keV, at a dose of 1×10^{15} cm^{-2}. All implants were performed with 0-degree tilt/rotation, through a thin screening oxide layer (2 nm SiO_2) that also served to protect the surface from contamination during ion implantation. The ion implantation conditions

a)Electronic mail: xi.zhang@berkeley.edu

are chosen such that the projected range is less than 20 nm for all dopants.

A conventional lamp-heated rapid thermal annealing (RTA) tool (AccuThermo model AW610) was used to anneal wafer samples after ion implantation. The annealing recipe stabilizes the sample temperature for 10 s at 700 °C before controllably ramping up the temperature at a rate of approximately 116 C/s to 1050 °C for a duration less than 1 s (i.e., a "spike anneal" to minimize dopant diffusion while achieving a high level of dopant activation). It is worthwhile to note here that a faster temperature ramp-up rate of 300 °C/s has been found to be advantageous for reducing TED-induced effects[7] but was not possible with the tool used in this work.

The ability of the OI layers to withstand high-temperature processing is essential for them to effectively impede dopant diffusion. Figure 1(a) shows the oxygen (O) profiles obtained by secondary ion mass spectrometry (SIMS) analyses of OI wafer samples before and after RTA treatment, proving that the OI layers can withstand a 1050 °C spike anneal process.

Dopant out-diffusion during thermal annealing can be significant for ultra-shallow implants[16] and is undesirable for achieving source/drain extension regions with low sheet resistance. To mitigate this "dose loss", some samples were capped with an insulating layer prior to RTA treatment, either comprising of 10 nm-thick low-temperature oxide (LTO) formed by chemical vapor deposition (CVD) at 400 °C or 10 nm-thick silicon nitride (SiN_x) deposited by plasma-enhanced chemical vapor deposition (PECVD) at 200 °C.

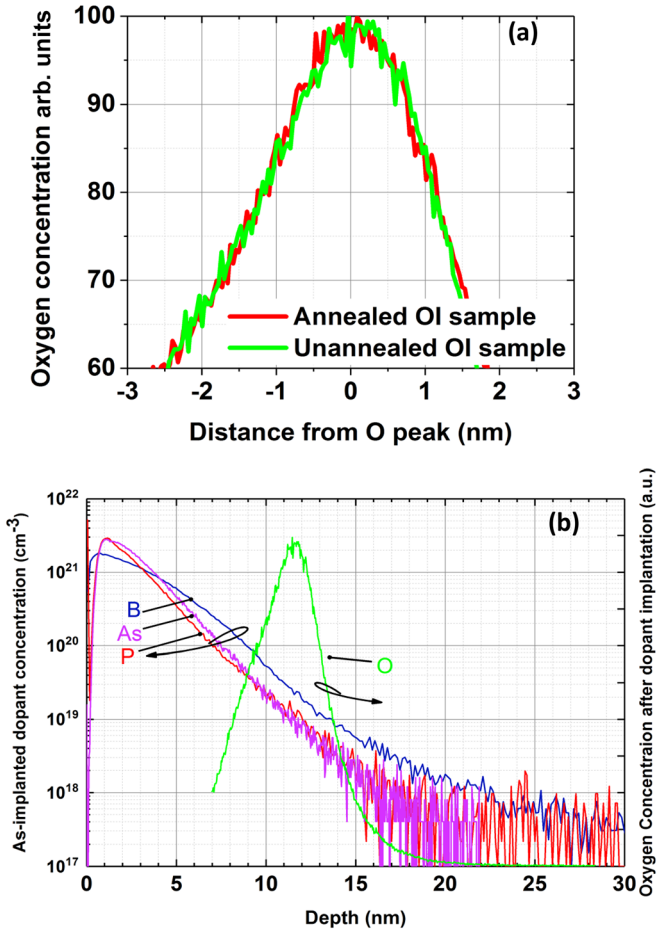

FIG. 1. Secondary ion mass spectrometry (SIMS) analyses: (a) oxygen profiles in OI samples. (b) Depth profiles of dopant concentration (log scale) and oxygen concentration (linear scale, arbitrary units) after dopant ion implantation.

TABLE I. Boron doses in control samples.

Sample	B dose ($\times 10^{14}$ cm^{-2})	Dose loss (%)
As-implanted	7.4	0
Uncapped	4.5	39
LTO capped	3.6	51
SiN_x capped	3.7	50

III. EXPERIMENTAL RESULTS

A. Dopant dose loss and diffusion in Si control samples

Table I shows the total B dose (calculated by integrating the B concentration profile obtained from SIMS) in the various B-doped control samples. It can be seen that 39% of the implanted B was lost from the annealed uncapped sample, as compared with the as-implanted sample. Neither the LTO capping layer nor the SiN_x capping layer helped to retain B. Furthermore, the B depth profiles in Fig. 2 show that the presence of a capping layer during the RTA treatment enhances B diffusion, perhaps due to strain-induced interstitial generation since diffusion of B is primarily interstitial-driven.[7] C_{enh}, defined as the concentration below which B diffusion is enhanced, can be seen to be approximately 1×10^{20} cm^{-3}, consistent with previous findings.[7] It is dependent on the intrinsic carrier concentration during the annealing process[7] and is not affected by the presence of a capping layer, as expected. The B concentration at the surface is similar for all three annealed samples, indicating negligible dopant segregation to the interface between the capping layer and the substrate.

Previous work[17–19] revealed that significant uphill diffusion (against the concentration gradient, i.e., toward the surface) occurs during thermal annealing, for shallowly implanted dopants. It was hypothesized that this is because the free surface

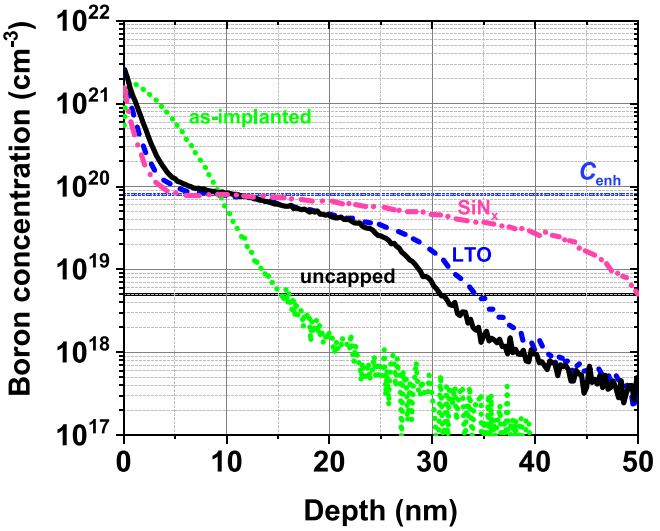

FIG. 2. Boron profiles in control Si samples, obtained using SIMS. C_{enh} is the same for uncapped and capped samples.

TABLE II. Phosphorus doses in control samples.

Sample	P dose ($\times 10^{14}$cm^{-2})	Dose loss (%)
As-implanted	7.5	0
Uncapped	2.2	70
LTO capped	3.6	52
SiN_x capped	3.2	57

TABLE III. Arsenic doses in control samples.

Sample	As dose ($\times 10^{14}$ cm^{-2})	Dose loss (%)
As-implanted	8.2	0
Uncapped	2.4	71
LTO capped	2.3	72
SiN_x capped	4.3	48

acts as a sink for interstitials[17,18] or dopant traps.[19] The results in Fig. 2 show that uphill diffusion occurred during the RTA treatment, for both uncapped and capped samples. This suggests that the interface between the capping layer and the substrate also acts as a sink for interstitials.

Table II shows the total P dose in the various P-doped control samples. It can be seen that 70% of the implanted P was lost from the annealed uncapped sample, as compared with the as-implanted sample. Both the LTO capping layer and the SiN_x capping layer helped to retain P during the RTA treatment. The P depth profiles in Fig. 3 clearly show that P uphill diffusion during the RTA treatment occurred in the uncapped sample. This phenomenon is less obvious in the capped samples due to their lower surface P concentration resulting from substantially enhanced diffusion into the substrate due to the aforementioned strain-induced interstitial generation.

Table III shows the total As dose in the various As-doped control samples. It can be seen that 71% of the implanted As was lost from the annealed uncapped sample, as compared with the as-implanted sample. Only the SiN_x capping layer helped to retain As during the RTA treatment. The As depth profiles in Fig. 4 show that the As profiles in the annealed samples are very shallow (note the smaller depth scale as compared with Figs. 1 and 2) thanks to the lower diffusivity of As *vs.* B and P. The presence of a capping layer does not significantly enhance As diffusion, which is primarily vacancy-driven.[6]

B. Effects of OI layers on dopant dose loss and diffusion

In advanced planar CMOSFETs (Complementary Metal Oxide Semiconductor Field Effect Transistors) the peak retrograde well dopant concentration is in the range of 10^{18} cm^{-3}. Therefore, in this study, the nominal junction depth (X_j) is taken to be the depth at which the (source/drain) dopant concentration falls to 5×10^{18} cm^{-3}. For a fair comparison of X_j values, only the dopant profiles for OI samples with a similar retained dopant dose as for the control sample should be compared. Figure 5 provides a comparison of B depth profiles for a control sample and for OI samples. It can be seen that B diffusion beyond the OI layers is effectively reduced because the diffusion of silicon self-interstitials beyond the OI layers is impeded. For a similar retained B dose, X_j is reduced by more than 50% in the OI sample. C_{enh} appears to be slightly higher in the OI samples, but the higher plateau is more likely due to a dopant pile-up effect[13] associated with the OI layers located at a depth of approximately 10 nm.

Figure 6 provides a comparison of P depth profiles for a control sample and an OI sample with a similar retained P dose. It can be seen that P diffusion beyond the OI layers is effectively reduced, so that X_j is reduced by 47% in the OI sample. The dopant pile-up effect in the region of the OI layers is also observed for P.

Figure 7 provides a comparison of As depth profiles for a control sample and an OI sample with a similar retained As dose. It can be seen that As diffusion beyond the OI layers is slightly reduced, so that X_j is reduced by 16% in the OI sample. Because As diffusion at 1050 °C is only 40% interstitial-driven,[6] the effect of the OI layers on As diffusion is less than for B and P diffusion.

Figures 8, 9, and 10 show the effects of the OI layers on dose retention and X_j after RTA treatment for B, P, and As, respectively. It can be seen that the OI layers are beneficial for

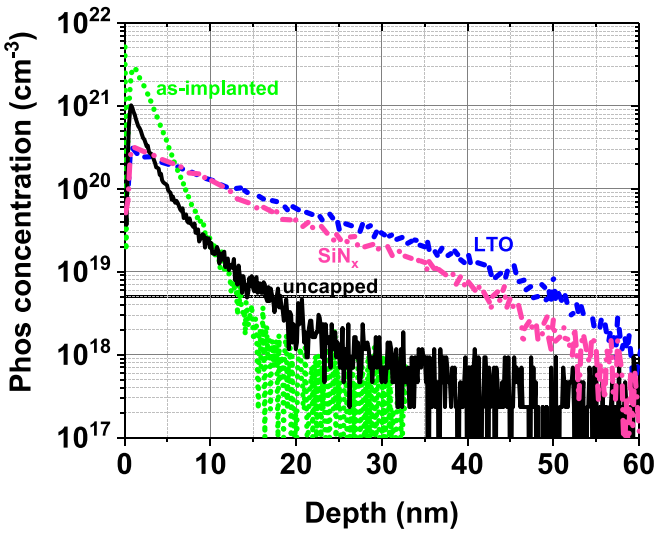

FIG. 3. Phosphorus profiles in control Si samples, obtained using SIMS.

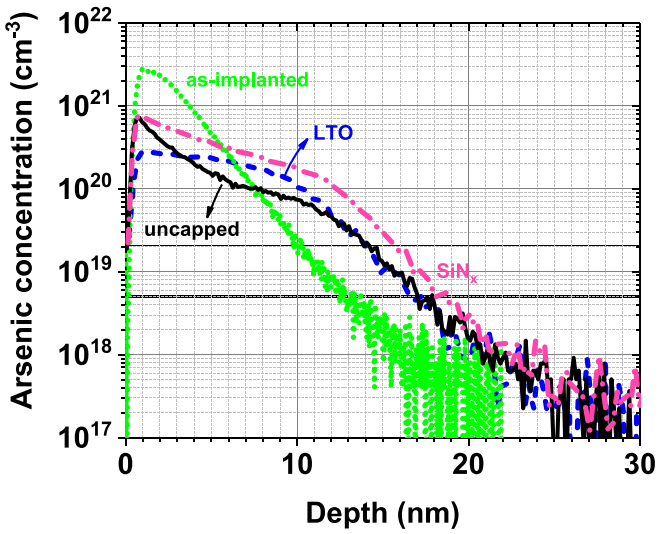

FIG. 4. Arsenic profiles in control Si samples, obtained using SIMS.

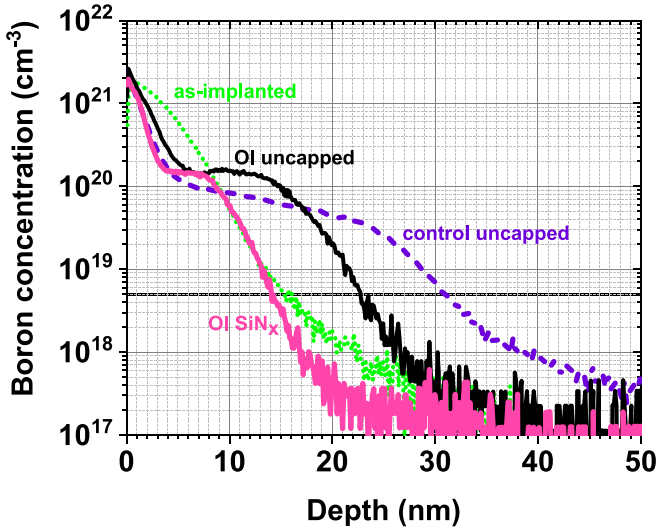

FIG. 5. Comparison of B profiles for control *vs.* OI samples. For the uncapped **control sample**, the retained B dose is 4.5×10^{14} cm^{-2} and $\mathbf{X_j = 31\,nm}$. For the SiN_x capped **OI sample**, the retained B dose is 4.6 $\times 10^{14}$ cm^{-2} and $\mathbf{X_j = 14\,nm}$. For the uncapped **OI sample**, the retained B dose is even higher, 6.2×10^{14} cm^{-2}, but the junction depth ($\mathbf{X_j = 22\,nm}$) is still shallower than for the uncapped control sample.

achieving shallower junction depth, in all cases. The OI layers also help to retain B. P out-diffusion for a SiN_x-capped sample is also reduced with OI layers. As out-diffusion for uncapped and LTO-capped samples is reduced with OI layers. The sheet resistance (R_{sh}) contour plots in these figures were generated using Sentaurus technology computer-aid design (TCAD) simulations[20,21] assuming a step function doping profile and 100% dopant activation rate. They suggest that the OI layers can provide for lower R_{sh}.

IV. SHEET RESISTANCE SIMULATIONS

Electrical activation of dopants is a complex phenomenon and can be affected by precipitation, clustering, and segregation.[22–24] Pulsed laser annealing can be used to increase

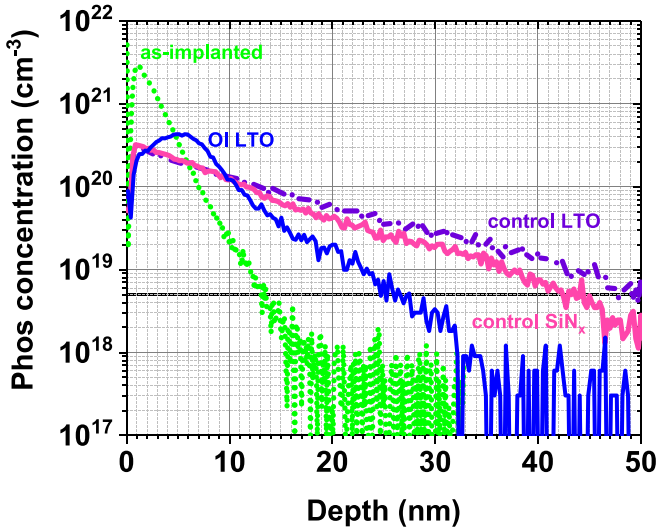

FIG. 6. Comparison of P profiles for control *vs.* OI samples. For the LTO-capped **control sample**, the retained P dose is 3.6×10^{14} cm^{-2} and $\mathbf{X_j = 49\,nm}$. For the LTO-capped **OI sample**, the retained P dose is 3.4 $\times 10^{14}$ cm^{-2} and $\mathbf{X_j = 26\,nm}$.

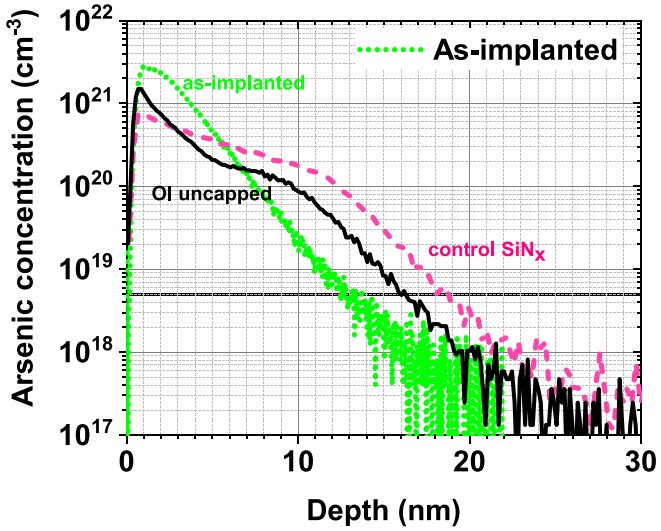

FIG. 7. Comparison of As profiles for control *vs.* OI samples. For the SiN_x-capped **control sample**, the retained As dose is 4.3×10^{14} cm^{-2} and $\mathbf{X_j = 19\,nm}$. For the uncapped **OI sample**, the retained As dose is 4.0 $\times 10^{14}$ cm^{-2} and $\mathbf{X_j = 16\,nm}$.

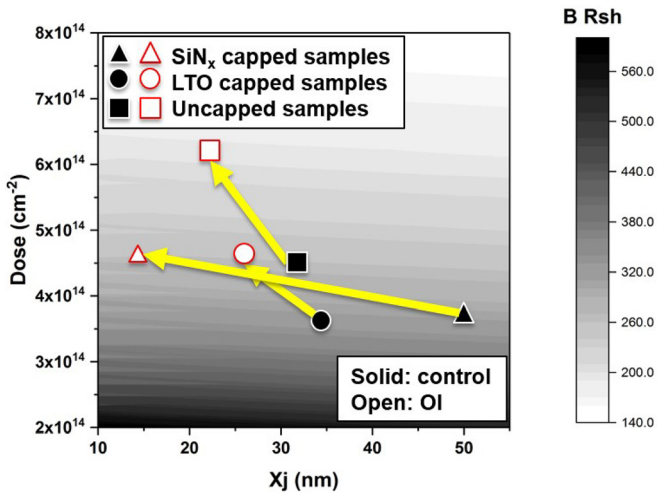

FIG. 8. Impact of OI layers on dopant retention and junction depth, for ultra-shallow junctions formed by B ion implantation.

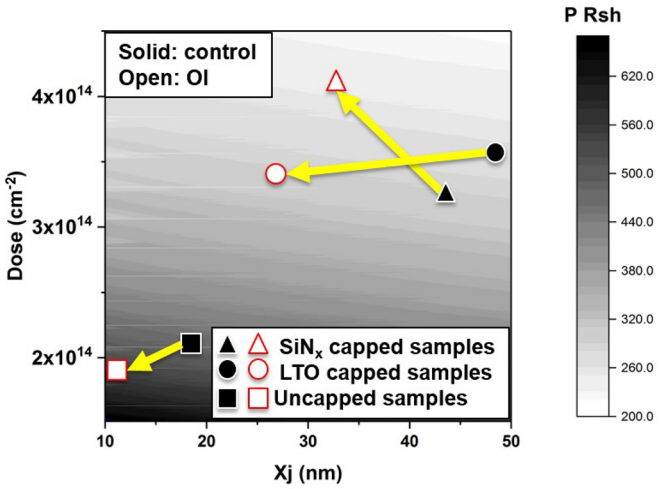

FIG. 9. Impact of OI layers (indicated by the arrows, each pointing from the control sample case to the OI sample case) on dopant retention and junction depth, for ultra-shallow junctions formed by P ion implantation.

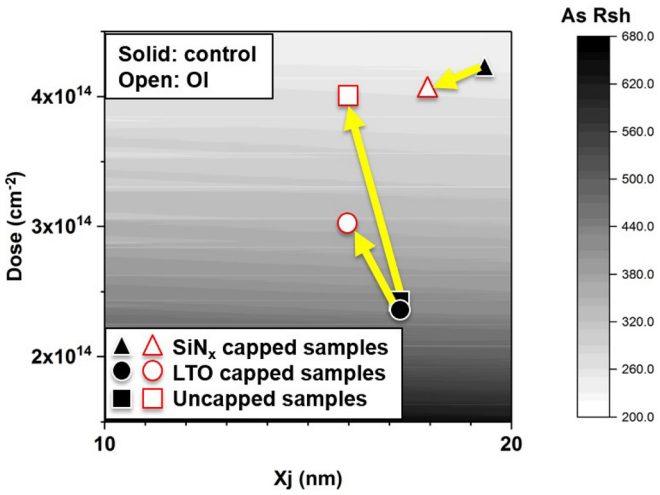

FIG. 10. Impact of OI layers (indicated by the arrows, each pointing from the control sample case to the OI sample case) on dopant retention and junction depth, for ultra-shallow junctions formed by As ion implantation.

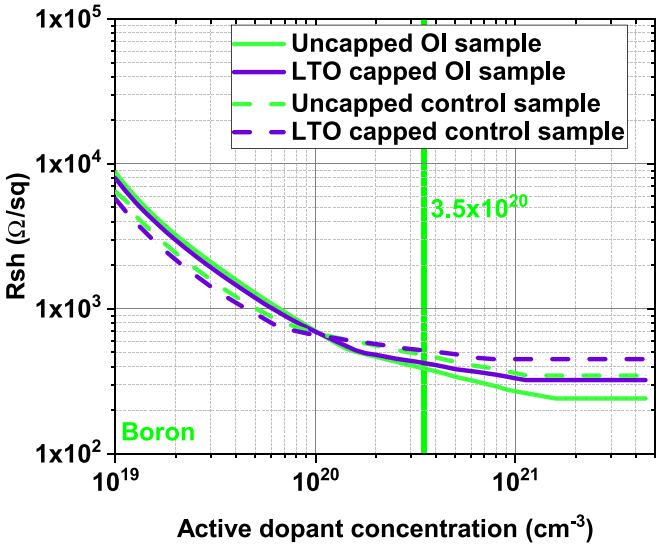

FIG. 11. R_{sh} *vs.* max active dopant concentration for boron-implanted samples.

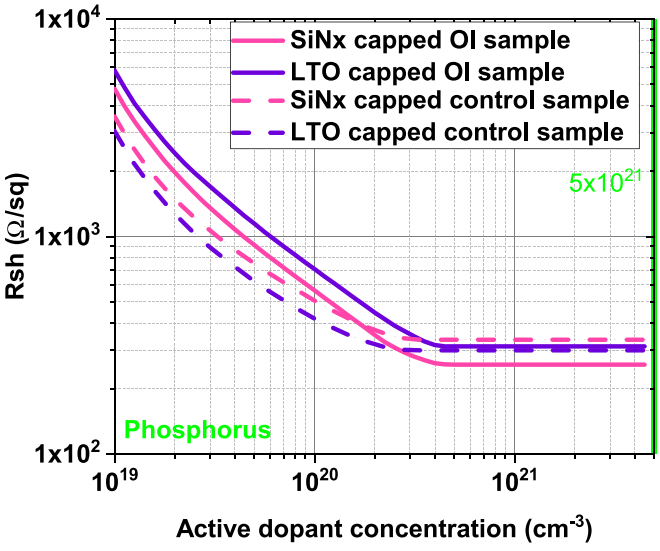

FIG. 12. R_{sh} *vs.* max active dopant concentration for phosphorus-implanted samples.

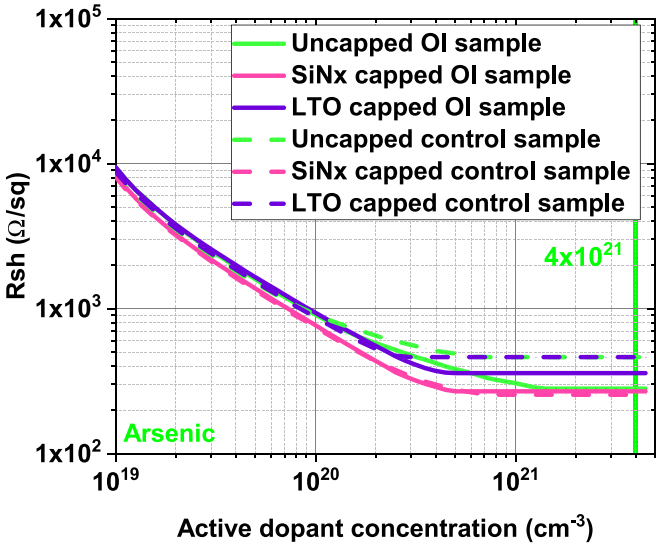

FIG. 13. R_{sh} *vs.* max active dopant concentration for arsenic-implanted samples.

the concentration of electrically active dopants in silicon and thereby lower R_{sh}.[22,23,25] Figures 11, 12 and 13 show the dependence of simulated R_{sh} on the maximum concentration of electrically active dopants, obtained using the dopant depth profiles from SIMS analyses.[21] In each of these figures, the vertical green lines demarcate the maximum reported electrically active dopant concentration.[22,23,25] It can be seen from a comparison of the curves for the OI samples *vs.* the control samples that the OI layers can be expected provide for lower R_{sh} at the maximum active doping level.[22,23,25] Therefore, OI technology should be beneficial for achieving shallower junctions with lower sheet resistance to enable further miniaturization of planar metal-oxide-semiconductor field-effect transistors for improved integrated-circuit performance and cost per function.

V. SUMMARY

In summary, the effects of OI layers on the diffusion of B, P, and As in silicon have been investigated, for ultra-shallow junction formation by high-dose ion implantation followed by spike annealing at 1050 °C. The OI layers are beneficial because they impede the diffusion of Si self-interstitials so that dopant diffusion beyond the depth of the OI layers is reduced. The OI layers can also help to retain more dopants within the Si, which should be beneficial for achieving ultra-shallow source/drain extension regions with high active dopant concentration. Fabrication and characterization of planar short-channel MOSFETs is necessary to experimentally verify the benefit of OI layers for improving transistor scalability and performance.

[1]L. Ho, in *2017 Third Quarter Earnings Conference* (Taiwan Semiconductor Manufacturing Company (TSMC), 2017).
[2]R. H. Dennard *et al.*, "Design of ion-implanted MOSFET's with very small physical dimensions," IEEE J. Solid-State Circuits **9**(5), 256–268 (1974).

[3]T. Yuan, C. H. Wann, and D. J. Frank, "25 nm CMOS design considerations," in Technical Digest - International Electron Devices Meeting, 1998, IEDM'98 (IEEE, 1998).
[4]T. Ghani *et al.*, "Scaling challenges and device design requirements for high performance sub-50 nm gate length planar CMOS transistors," in Digest of Technical Papers - 2000 Symposium on VLSI Technology, 2000 (IEEE, 2000).
[5]P. M. Fahey, P. B. Griffin, and J. D. Plummer, "Point defects and dopant diffusion in silicon," Rev. Mod. Phys. **61**(2), 289 (1989).
[6]B. Hartmut, "Diffusion mechanisms and intrinsic point-defect properties in silicon," MRS Bull. **25**(6), 22–27 (2000).
[7]S. C. Jain *et al.*, "Transient enhanced diffusion of boron in Si," J. Appl. Phys. **91**(11), 8919–8941 (2002).
[8]S. Mirabella *et al.*, "Mechanisms of boron diffusion in silicon and germanium," J. Appl. Phys. **113**, 031101 (2013).
[9]S. M. Hu, P. Fahey, and R. W. Dutton, "On models of phosphorus diffusion in silicon," J. Appl. Phys. **54**(12), 6912–6922 (1983).
[10]F. F. Morehead and R. F. Lever, "Enhanced "tail" diffusion of phosphorus and boron in silicon: Self-interstitial phenomena," Appl. Phys. Lett. **48**(2), 151–153 (1986).
[11]S. Solmi *et al.*, "Transient enhanced diffusion of arsenic in silicon," J. Appl. Phys. **94**(8), 4950–4955 (2003).
[12]N. Xu *et al.*, "Extension of planar bulk n-channel MOSFET scaling with oxygen insertion technology," IEEE Trans. Electron Devices **61**(9), 3345–3349 (2014).
[13]R. J. Mears *et al.*, "Punch-through stop doping profile control via interstitial trapping by oxygen-insertion silicon channel," in Electron Devices Technology and Manufacturing Conference (EDTM) (IEEE, 2017), pp. 65–66.
[14]H. S. Chao *et al.*, "Species and dose dependence of ion implantation damage induced transient enhanced diffusion," J. Appl. Phys. **79**(5), 2352–2363 (1996).
[15]D. Boyd *et al.*, "Ultra-thin body super-steep retrograde well (SSRW) FET devices," U.S. patent No. 20060022270A1 (30 July 2004).
[16]S. Ruffell, I. V. Mitchell, and P. J. Simpson, "Annealing behavior of low-energy ion-implanted phosphorus in silicon," J. Appl. Phys. **97**(12), 123518 (2005).
[17]R. Duffy *et al.*, "Boron uphill diffusion during ultrashallow junction formation," Appl. Phys. Lett. **82**(21), 3647–3649 (2003).
[18]H. C.-H. Wang *et al.*, "Interface induced uphill diffusion of boron: An effective approach for ultrashallow junction," IEEE Electron Device Lett. **22**(2), 65–67 (2001).
[19]M. Ferri *et al.*, "Arsenic uphill diffusion during shallow junction formation," J. Appl. Phys. **99**(11), 113508 (2006).; D.-W. Lin *et al.*, "A constant-mobility method to enable MOSFET series-resistance extraction," IEEE Electron Device Lett. **28**(12), 1132–1134 (2007).
[20]D. A. Antoniadis *et al.*, "Boron in near-intrinsic ⟨100⟩ and ⟨111⟩ silicon under inert and oxidizing ambients—diffusion and segregation," J. Electrochem. Soc. **125**(5), 813–819 (1978).
[21]Sentaurus Device User Guide, Version N, Synopsys Inc., Mountain View, CA, USA, 2017.
[22]D. Nobili *et al.*, "Precipitation as the phenomenon responsible for the electrically inactive phosphorus in silicon," J. Appl. Phys. **53**(3), 1484–1491 (1982).
[23]S. Solmi *et al.*, "High-concentration boron diffusion in silicon: Simulation of the precipitation phenomena," J. Appl. Phys. **68**(7), 3250–3258 (1990).
[24]R. Turan *et al.*, "Mapping electrically active dopant profiles by field-emission scanning electron microscopy," Appl. Phys. Lett. **69**(11), 1593–1595 (1996).
[25]D. Nobili *et al.*, "Precipitation as the phenomenon responsible for the electrically inactive arsenic in silicon," J. Electrochem. Soc. **130**(4), 922–928 (1983).